AFRL-ML-WP-TP-2006-481

MICROSTRUCTURE AND TEMPERATURE EFFECTS ON THE FATIGUE VARIABILITY BEHAVIOR OF AN α+β TITANIUM ALLOY AND IMPLICATIONS FOR LIFE PREDICTION (POSTPRINT)

Sushant K. Jha, James M. Larsen, and Andrew H. Rosenberger

FEBRUARY 2006

Approved for public release; distribution is unlimited.

STINFO COPY

MATERIALS AND MANUFACTURING DIRECTORATE
AIR FORCE RESEARCH LABORATORY
AIR FORCE MATERIEL COMMAND
WRIGHT-PATTERSON AIR FORCE BASE, OH 45433-7750

REPORT DOCUMENTATION PAGE

Form Approved
OMB No. 0704-0188

1. REPORT DATE *(DD-MM-YY)*	2. REPORT TYPE	3. DATES COVERED *(From - To)*
February 2006	Conference Paper Postprint	

4. TITLE AND SUBTITLE
MICROSTRUCTURE AND TEMPERATURE EFFECTS ON THE FATIGUE VARIABILITY BEHAVIOR OF AN α+β TITANIUM ALLOY AND IMPLICATIONS FOR LIFE PREDICTION (POSTPRINT)

5a. CONTRACT NUMBER
In-house

5b. GRANT NUMBER

5c. PROGRAM ELEMENT NUMBER
62102F

6. AUTHOR(S)
Sushant K. Jha (Universal Technology Corporation)
James M. Larsen and Andrew H. Rosenberger (AFRL/MLLMN)

5d. PROJECT NUMBER
M02R

5e. TASK NUMBER
30

5f. WORK UNIT NUMBER
00

7. PERFORMING ORGANIZATION NAME(S) AND ADDRESS(ES)

Universal Technology Corporation Dayton, OH 45432	Metals Branch, Behavior/Life Prediction Section (AFRL/MLLMN) Metals, Ceramics, and Nondestructive Evaluation Division Materials and Manufacturing Directorate Air Force Research Laboratory, Air Force Materiel Command Wright-Patterson Air Force Base, OH 45433-7750

8. PERFORMING ORGANIZATION REPORT NUMBER
AFRL-ML-WP-TP-2006-481

9. SPONSORING/MONITORING AGENCY NAME(S) AND ADDRESS(ES)
Materials and Manufacturing Directorate
Air Force Research Laboratory
Air Force Materiel Command
Wright-Patterson AFB, OH 45433-7750

10. SPONSORING/MONITORING AGENCY ACRONYM(S)
AFRL-ML-WP

11. SPONSORING/MONITORING AGENCY REPORT NUMBER(S)
AFRL-ML-WP-TP-2006-481

12. DISTRIBUTION/AVAILABILITY STATEMENT
Approved for public release; distribution is unlimited.

13. SUPPLEMENTARY NOTES

Conference paper proceedings published in the 9th International Fatigue Congress (Fatigue 2006 Proceedings), Elsevier Ltd, publisher. This paper contains color. PAO Case Number: AFRL/WS 06-0545; clearance date: 27 Feb 2006.

14. ABSTRACT
We have studied the effects of microstructure and temperature on the fatigue variability behavior of the α+β titanium alloy, Ti-6Al2Zr-4Sn-6Mo (Ti-6-2-4-6). These variables had separate influence on the minimum, and the mean behavior. This was related to perhaps a fundamental aspect of fatigue variability which dictates that at any stress level, the mean is dominated by a mechanism different from the one controlling the lower-tail behavior. As a result in this material, while the mean response was increasingly dominated by the crack initiation regime with decreasing stress level (which is the conventionally expected behavior), at the same time the life-limiting behavior was controlled by the crack growth regime. This produced a very systematic effect of microstructure and temperature on total uncertainty in lifetime depending on the sensitivity of crack initiation and growth regimes to these variables. We suggest a new paradigm to treat the fatigue variability behavior and show that, this can have significant implications for life management especially, with respect to reducing the uncertainty with life prediction and improving the reliability of design life.

15. SUBJECT TERMS
Fatigue variability, α+β titanium, Ti-6AI-2Sn-4Zr-6Mo, Life prediction, Crack initiation, Crack growth, Probability of failure, Microstructure

16. SECURITY CLASSIFICATION OF:			17. LIMITATION OF ABSTRACT:	18. NUMBER OF PAGES	19a. NAME OF RESPONSIBLE PERSON (Monitor)
a. REPORT	b. ABSTRACT	c. THIS PAGE			Andrew H. Rosenberger
Unclassified	Unclassified	Unclassified	SAR	18	19b. TELEPHONE NUMBER *(Include Area Code)* N/A

Standard Form 298 (Rev. 8-98)
Prescribed by ANSI Std. Z39-18

ORAL REFERENCE: FT493

MICROSTRUCTURE AND TEMPERATURE EFFECTS ON THE FATIGUE VARIABILITY BEHAVIOR OF AN α+β TITANIUM ALLOY AND IMPLICATIONS FOR LIFE PREDICTION

S. K. Jha[1], J. M. Larsen, and A. H. Rosenberger

US Air Force Research Laboratory, Wright-Patterson AFB, Dayton, OH 45431, USA
[1]Universal Technology Corporation, Dayton, OH 45432, USA

ABSTRACT

We have studied the effects of microstructure and temperature on the fatigue variability behavior of the α+β titanium alloy, Ti-6Al-2Zr-4Sn-6Mo (Ti-6-2-4-6). These variables had separate influences on the minimum, and the mean fatigue behavior. This appeared to be related to a fundamental aspect of fatigue variability which dictates that at any stress level, the mean is dominated by a mechanism different from the one controlling the lower-tail behavior. As a result in this material, while the mean fatigue-lifetime response was increasingly dominated by the crack initiation regime with decreasing stress level (which is the conventionally expected behavior), at the same time the life-limiting behavior was controlled by the crack growth regime. This produced a very systematic effect of microstructure and temperature on total uncertainty in lifetime, depending on the sensitivity of crack initiation and growth regimes to these variables. We suggest a new paradigm to treat the fatigue variability behavior and show that this can have significant implications for life management, especially with respect to reducing the uncertainty with life prediction and improving the accuracy of design life.

KEYWORDS

Fatigue variability, α+β titanium, Ti-6Al-2Sn-4Zr-6Mo, Life prediction, Crack initiation, Crack growth, Probability of failure, Microstructure

INTRODUCTION

Material design has traditionally been based on the conventionally expected response of the mean fatigue behavior to the material and operating variables [1]. Similarly, component life management is driven by lifetime variability about the overall mean behavior [2]. This approach is understandable given the strong relationship of the mean lifetime with microstructure, stress state, and other loading variables. These correlations have been studied extensively in many material systems [1] and a general understanding of the mean fatigue behavior with respect to these variables has been developed. The treatment of the fatigue variability behavior, which is more important from the design-life perspective, is also guided by this understanding [3, 4]. Therefore, most studies of fatigue variability seek to determine the uncertainty about the mean as induced by distribution in, for example, the microstructural variables [5, 6]. However, in several materials, we find that the quite valid understanding of the mean behavior may not be suitable for treating effects of key parameters on the fatigue variability behavior. We reported earlier [7-10], and also in this

proceedings [11], that the total uncertainty in lifetime at given stress level was due to superposition of variability associated with at least two mechanisms, such that the life-limiting (or the worst-case) mechanism was controlled by the small + long crack growth variability, while the longer life mechanism followed the conventionally expected behavior. Therefore with decreasing stress level, although the mean fatigue lifetime was dominated by the conventionally expected response, the minimum (worst-case) behavior was controlled by a different mechanism. This resulted in increased separation between the mechanisms at lower stress levels [7], therefore increasing the total variability. Although this type of separation of mean and the worst-case behavior may not be seen in all cases, depending on the number of tests, and the degree of overlap between lifetimes [11], the theoretical possibility of this behavior needs to be assessed probabilistically. We suggest that a new paradigm is required to describe the general fatigue variability behavior of many structural materials. This is especially critical with respect to the design-life prediction.

In this paper, we discuss the above issues with reference to the α+β titanium alloy, Ti-6-2-4-6. This class of titanium alloys is used in turbine engine applications up to intermediate temperature levels [12, 13]. The service life of these components is limited by fatigue, and the fatigue variability is one of the most important considerations in the design life [2, 14]. However, although there are innumerable studies on the fatigue of titanium alloys [15-18] and titanium based materials [19, 20], there has been limited study of their fatigue variability behavior. As noted above, this may be due to the general acceptability that the conventional understanding of the mean fatigue response is also applicable to the variability behavior. We attempt to develop a physically based understanding of the fatigue variability behavior and propose an alternate paradigm to treat this aspect of fatigue. We discuss the applicability of the paradigm with respect to the fatigue variability response to microstructure and temperature. The potential effect of the proposed framework on the uncertainty associated with the traditional approach to life prediction and the reliability of design life is also discussed.

MATERIALS AND EXPERIMENTAL PROCEDURE

Materials

The material in this study was an α+β titanium alloy, Ti-6Al-2Sn-4Zr-6Mo. Two different heats of the material with different thermomechanical work levels were considered. These are referred to as the pancake forging and the disk material and their microstructures are shown in Fig. 1 (a) and (b) respectively. As shown, the microstructures were very similar in appearance and consisted of equiaxed primary α (α_p) grains and lath α in transformed prior-β grains. The α_p area fractions measured in random sections of the pancake and the disk material were about 19% and 33% respectively. The aspect ratio of lath α was larger in the pancake than the disk and was about 1.87 and 1.45 respectively. The microstructures differed significantly in terms of their texture as illustrated by the pole figures in Fig. 1.

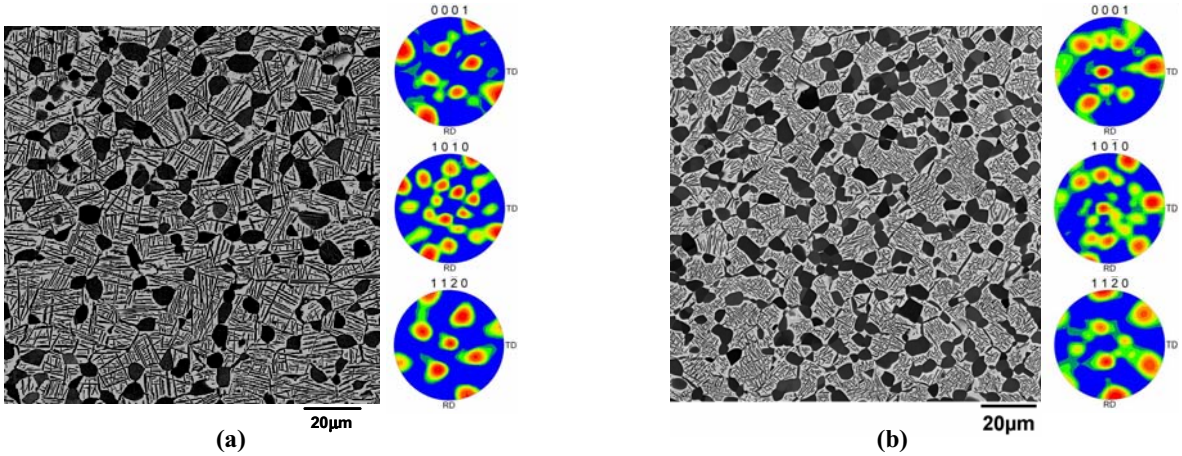

Figure 1: Microstructures of the two heats of the Ti-6-2-4-6 alloy; (a) the pancake, and (b) the disk material.

Experimental

The fatigue specimens were electro-discharge machined from the forgings of the two heats of the material. The final machining step involved low stress grinding. Subsequently, each specimen was electropolished (to remove approximately 50 μm from the surface) to eliminate the surface residual stress and to produce a uniform surface condition. Specimens had a round-bar geometry with a uniform gage length of about 12.5 mm and a diameter of about 4 mm. The fatigue tests were conducted using an MTS 810 servo hydraulic test system equipped with a 458 controller. The experiments were performed in load-control in lab air at room temperature and 260ºC. The stress ratio was 0.05, and the frequency was 20 Hz. For the elevated temperature experiments, a button-head specimen geometry similar to the one described in [10] was used. The gage section was kept the same as in the room temperature specimens. A resistance-heated furnace with dual zone temperature control was mounted on the MTS frame for this purpose. Control thermocouples were welded to two locations near the gage of the sample and the temperature was maintained within ± 2ºC of the set point.

The small-crack growth was monitored using the acetate replication technique. Cracks initiating from starter notches, as well as those naturally initiating, were studied. Starter notches were machined using the Femtosecond laser at the University of Michigan, the details of which can be found elsewhere [21]. Additionally, notches were machined in some samples using a Focused Ion Beam (FIB). Replicas were recorded at predetermined cycle intervals at the static load of 60% of the maximum load in a cycle.

Fractography and orientation imaging microscopy (OIM) were performed in a Cambridge S360FE scanning electron microscope. The microscope was equipped with a TSL OIM system. For imaging, the accelerating voltage of 15 kV and the probe current of 100 pA was used. For OIM, the accelerating voltage and the probe current of 20 kV and 10 nA were employed. The sample was tilted at 70º with respect to the horizontal axis, and the working distance was 25 mm. The sample was moved in steps in automated stage control to scan a large area in single session.

RESULTS AND DISCUSSION

Fatigue Variability Behavior of the Pancake Material

The room temperature fatigue variability behavior of the pancake material is presented in Fig. 2. As shown in Fig. 2(a), with decreasing stress level, the uncertainty in lifetimes increased to up to more than two orders in magnitude. While the mean behavior followed the conventionally expected response to stress level, the minimum lifetime did not vary much, as illustrated by Fig. 2(b). This indicates that the mean and the lower tail behavior may be governed by different mechanisms. This was more evident when the experimental points were plotted in the Cumulative Distribution Function (CDF) coordinates. A detailed discussion of this behavior has been provided elsewhere [7], and a few examples are reproduced in Fig. 2(c).

The CDF plots for stress levels (σ_{max}) of 1040 and 860 MPa are presented in Fig. 2(c). As shown, while the CDF matched well with the data at 1040 MPa, the agreement was very poor at 860 MPa. Further, at 860 MPa, the experimental points showed a step-like shape (illustrated by dashed lines) with respect to the CDF. This is another indication of superposition of two mechanisms [7] at the same stress level. Therefore, the total uncertainty in lifetime may be due to superposition of variability associated with these mechanisms, designated as Type I (life on the order of 10^4 cycles) and Type II (life on the order of 10^6 cycles) in the figure. The significant increase in variability with decreasing stress level can therefore be attributed to increasing separation between the mechanisms as the stress level is decreased.

The total lifetime is thought to have increasing contribution of the crack initiation regime with decreasing stress level, especially in titanium alloys [22-24]. This is perhaps, also true for the mean behavior in the present case. However, our results suggest that, this effect is produced due to increasing domination of the Type II mechanism on the mean lifetime as the stress level is decreased. Therefore, applying the traditional understanding of the mean response to describing the fatigue variability, i.e., in terms of the variability about the overall mean behavior may not be accurate in this case.

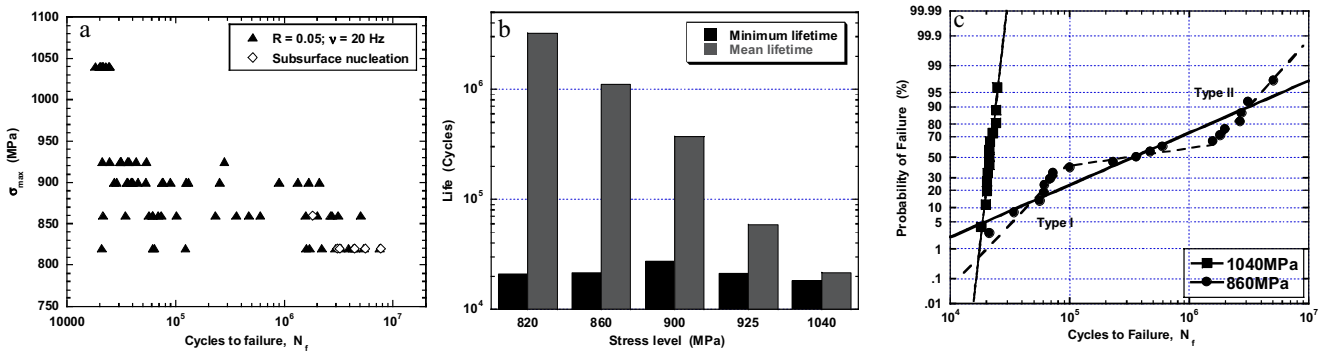

Figure 2: Fatigue variability behavior of the pancake microstructure; (a) Fatigue variability, (b) The minimum vs. the mean behavior with respect to stress level, and (c) Experimental points plotted in the CDF space illustrating good agreement between the CDF and data at 1040 MPa and a step-like shape of data points with respect to the CDF at 860 MPa.

Controlling Size Scale

It is important to assess the level of contribution to the lifetime variability arising at different material size scales. This will also provide insights into the fatigue regimes that control the variability. Based on the above discussion, we draw a distinction between the total variability i.e., dominated by separation between the two mechanisms, and the variability within a mechanism. The small-crack growth behavior from starter notches of different sizes, as well as from natural initiation was studied, and results are presented in Fig. 3 (a). The starting sizes are indicated in the figure. The notches were machined using the Femtosecond laser [21] and FIB, and their morphology is reveled at the crack origins in the failed samples shown in Figs. 3 (b) and (c), respectively. Clearly the small-crack effect, which would indicate a deviation from the continuum or the Linear Elastic Fracture Mechanics (LEFM) controlled crack growth, was not seen when the starting size was 20 X 25 μm^2 or greater. Further, there was no significant variability between the crack growth behavior of the notched samples and their data matched with the long-crack curve obtained using a C(T) sample. On the other hand, a significant small-crack effect was observed when crack initiated naturally in an equiaxed α grain of about 4 μm size. An image of the surface replica of the naturally initiated crack recorded at N = 20,000 is shown in Fig. 3(d). This indicates that, most of the contribution to fatigue variability seen in the S-N plot (Fig. 2(a)) originated in crack initiation and small crack growth occurring on the order of the equiaxed α_p size (< about 20 – 30 μm).

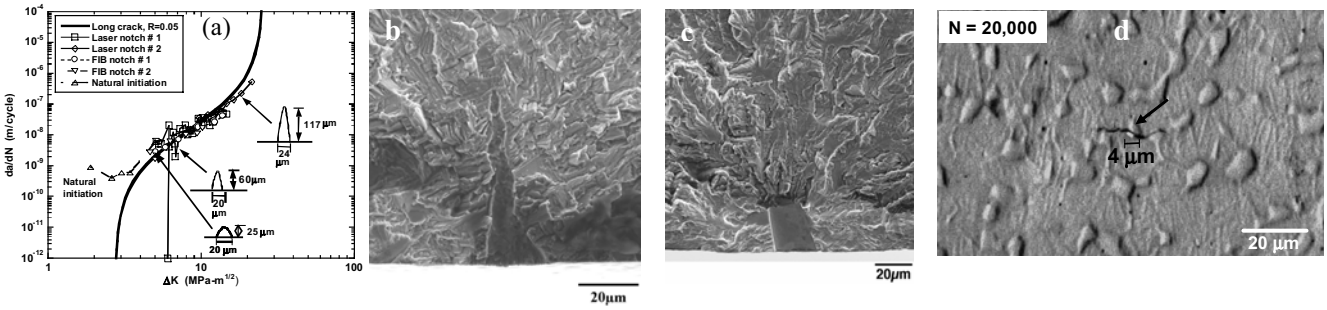

Figure 3: Illustration of the fatigue variability controlling size scale in Ti-6-2-4-6; (a) small-crack growth behavior, (b) example of a femtosecond laser machined notch, (c) a FIB machined notch, and (d) naturally initiated small crack recorded at N = 20,000 cycles (N_f = 39,864).

Total Variability vs. Variability within a Mechanism

Crack Initiation Characteristics

As discussed above, the study into the controlling size scale revealed that the maximum contribution to fatigue variability originated from crack initiation and early small-crack growth. The question remains as to how these contributions break down into the separation of mechanisms and the variability in the worst-case mechanism (i.e., Type I). As shown in Fig. 3(d), crack initiation occurred across one (or more) equiaxed α grain, irrespective of lifetime. This produced a facet (or facets) corresponding to the crack initiation plane, as shown in Fig. 4 (a). The size distribution of crack initiation facets, measured in failed samples, is compared to the nominal equiaxed α size distribution in Fig. 4(b). Although the crack initiation size distribution is displaced slightly towards larger values, it is not in the extreme right tail of the nominal α size distribution. It is to be noted that, while the nominal size distribution represents random α grain sections and therefore is biased towards smaller sizes, the crack initiation tends to occur across the largest plane in a grain [25]. This may account for part of the shift towards larger sizes. Nevertheless, it can be concluded that the size of the α grain is not the most critical criterion for crack initiation.

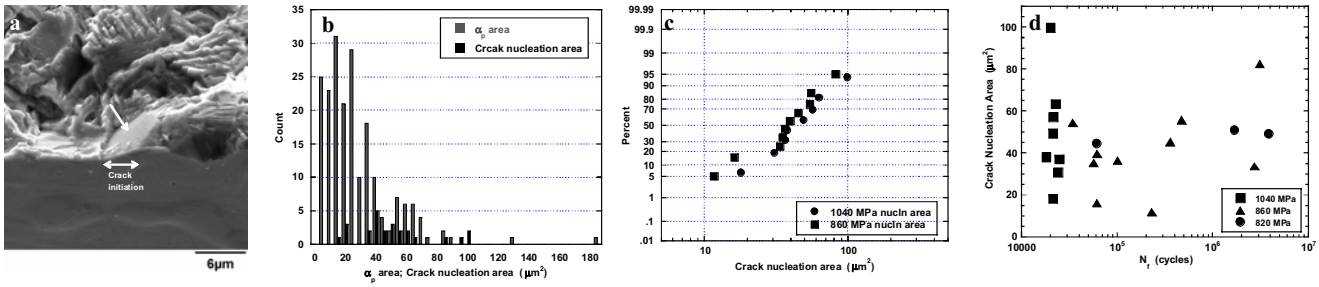

Figure 4: Crack initiation characteristics in the pancake microstructure; (a) typical crack initiation facet (the sample, shown at 45º tilt, is the same as shown in Fig. 5(d) and had the lifetime of 39,864 cycles), (b) crack initiation area distribution compared to the nominal α_p area distribution, (c) comparison of variability in the crack initiation area with respect to stress level, and (d) crack initiation size vs. lifetime.

The variability in the crack initiation sizes at 1040 and 860 MPa are compared in Fig. 4(c). Clearly, the mean crack initiation size, as well the scale of variability is similar at both stress levels, indicating no dependence of crack initiation size on the stress level. The crack initiation area with respect to lifetime is plotted in Fig. 4(d) and once again, no apparent correlation with the total variability in lifetime is observed. For example at 860 MPa, while the lifetime varied by two orders of magnitude, the crack initiation area for each of the measured samples remained almost the same. Also, given the high volume fraction of α_p, there is almost 100% probability of finding an α_p with the right orientation for crack initiation in the specimen surface [26]. Therefore, the separation between mechanisms and the total variability was not caused only by the size or the orientation of the crack initiating α grain. This, points towards the critical role of the crack initiation neighborhood and its relationship to the local deformation in causing the total variability.

With decreasing stress level, the crack initiation lifetime increases and is expected to dominate the total lifetime [22-24]. The Type II failures also follow the same trend with stress level, indicating significant contribution of the crack initiation regime in their lifetimes. We also show in the next section that, the crack growth lifetime may be relatively insignificant when compared to the total lifetime of the Type II failures and cannot account for the more than two orders of magnitude variability at lower stress levels. The separation between Type I and II mechanisms may, therefore, be related to the increasing crack initiation life of the Type II failures with decreasing stress level. It is to be noted that, several definitions of crack initiation are employed in literature depending on the material and the problem being examined [27, 28]. In the present study, we define crack initiation as the formation of a crack across an equiaxed α grain and the onset of its propagation.

Role of Small-Crack Growth in Fatigue Variability

As noted above, the separation of mechanisms, and therefore the total variability, seems to be dominated by the crack initiation regime at lower stress levels. However, lifetimes of the Type I failures indicate that the variability in this mechanism may be related to crack growth. Bounds on the crack growth lifetime can be calculated based on the limiting crack initiation sizes and the upper and the lower bounds on small-crack

growth rates. Since the small-crack data from only one naturally initiated crack was available, the limiting small-crack growth curves were assumed to be described by the experimentally measured behavior (Fig. 3(a)) and the extrapolation of the Paris-regime of the long-crack growth curve. This is illustrated in Fig. 5(a). The stress intensity (K) solution for elliptical surface crack in a solid cylinder formulated in [29] was used. The calculated bounds on crack growth lifetime are plotted in the S-N space in Fig. 5(b). As shown, the variability in lifetimes of the Type I failures are described by the crack growth bounds, indicating that the Type I mechanism was controlled by small + long crack growth starting from the equiaxed α size scale. Since the Type II failure lifetimes were largely governed by crack initiation, these could not be accounted for by the present calculations.

Assessing the Effects of Microstructure and Temperature on Fatigue Variability

Microstructure

The effect of microstructure on the fatigue variability behavior is shown in Fig. 6. In this figure, the behavior of the disk material is compared to that of the pancake microstructure at σ_{max} levels of 860 (Fig. 6(a)) and 820 MPa (Fig. 6(b)). Firstly, we find a step-like shape of the disk data points with respect to the CDF at both stress levels, which is consistent with the behavior of the pancake microstructure. Secondly, a shift in the Type II lifetimes of the disk microstructure can be seen at both stresses, as indicated in the figures. At the same time, there is almost no effect of microstructure on the Type I distribution. These factors led to a decrease in both the mean and the total variability in lifetime of the disk microstructure when compared to the pancake material.

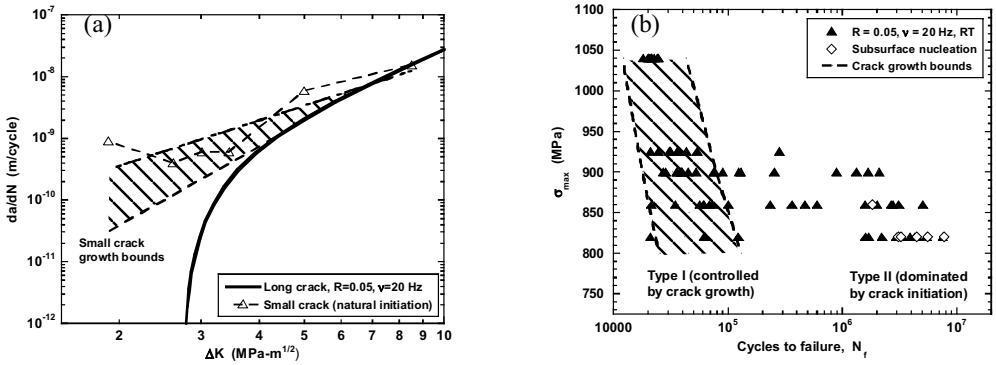

Figure 5: Bounds on small + long crack growth lifetimes; (a) the range in small-crack growth rates, and (b) the calculated bounds on crack growth lifetimes.

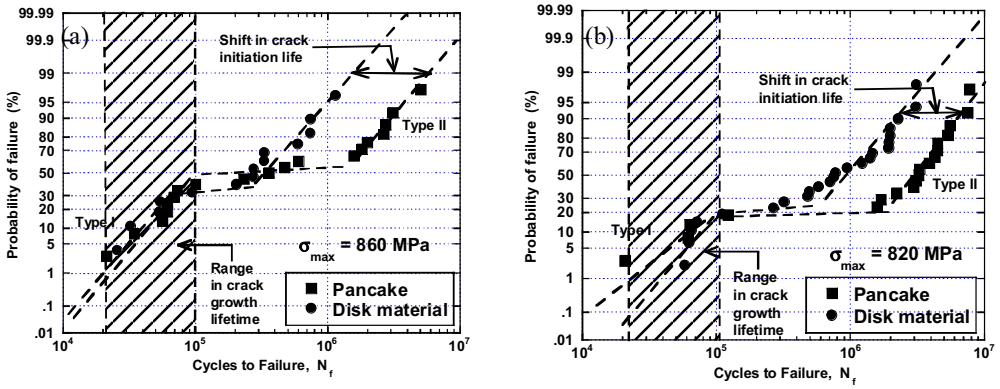

Figure 6: Effect of microstructure on the fatigue variability behavior of Ti-6-2-4-6; (a) σ_{max} = 860 MPa, and (b) σ_{max} = 820 MPa.

The effect of microstructure shows remarkable consistency with the crack initiation vs. propagation related duality in fatigue variability, previously discussed with reference to the pancake microstructure. The shift in the Type II mechanism of the disk material can be attributed to the influence of microstructure on the crack initiation lifetime. Since the size or the orientation of individual α_p does not correlate with total fatigue

variability, the failure initiation is likely dependent on the crack initiation neighborhood especially, the heterogeneity in deformation caused by local crystallographic orientations [30]. Preliminary results of the orientation measurements at the crack initiation site upon sectioning by FIB revealed that, the crack initiating α_p grain had a near-basal orientation with respect to the loading axis, while the surrounding grains were favorably oriented for prism <a> type deformation [30]. Although the primary microstructural characteristics of the two heats of Ti-6-2-4-6 were very similar, their texture was significantly different as shown in Fig. 1. The relationship of this difference in texture to crack initiation lifetime is not clear at present. It can be suggested that more random distribution of basal α grains in case of the disk microstructure [31] may create more opportunities for critical sites for crack initiation, leading to shorter crack initiation lifetime.

The almost insignificant effect of microstructure on the Type I failure distribution is attributed to the similar crack growth behavior of the two microstructures [32]. The room temperature and the 260ºC crack growth behavior of the pancake material were obtained under high vacuum conditions (about 10^{-10} Torr). Once again, no significant effect on the crack growth behavior was produced between room temperature and 260ºC [32]. The range in calculated crack growth lifetimes is superimposed on the plots in Fig. 6. As shown, these crack growth bounds roughly describe the variability in the Type I mechanism.

Temperature

In Fig. 7(a), the fatigue variability behavior of the pancake and the disk microstructures at 260ºC are compared to their behavior at room temperature at the σ_{max} level of 860 MPa. It is not surprising that, since the crack growth behavior at the two temperatures is similar, the distributions in the Type I lifetimes are similar in all cases. However, once again there is a significant shift in the Type II mechanisms of both microstructures, presumably due to a much stronger sensitivity of the crack initiation regime to temperature. As a result, the mean and the total variability in lifetime are further decreased at the elevated temperature, although the minimum (and perhaps the variability) in the Type I failures remain largely unaffected.

The mean and the minimum fatigue-lifetime behavior with respect to microstructure and temperature at 860 MPa are shown in Fig. 7(b). As shown, at the same stress level, the microstructure and temperature have very strong effect on the mean behavior, but the minimum lifetime does not vary significantly. As noted previously, this is suggested to be due to the mean being dominated by the Type II mechanism at lower stress levels, while the minimum behavior is controlled by the Type I mechanism. In a traditional life prediction approach, the microstructure and external variables may be sources of increased uncertainty in design life. However, Figs. 7 (a and b) show that an improved understanding of fatigue variability can reveal a very systematic effect of microstructure and loading variables on the fatigue variability behavior that may afford an opportunity for reduced uncertainty and a more reliable design life prediction.

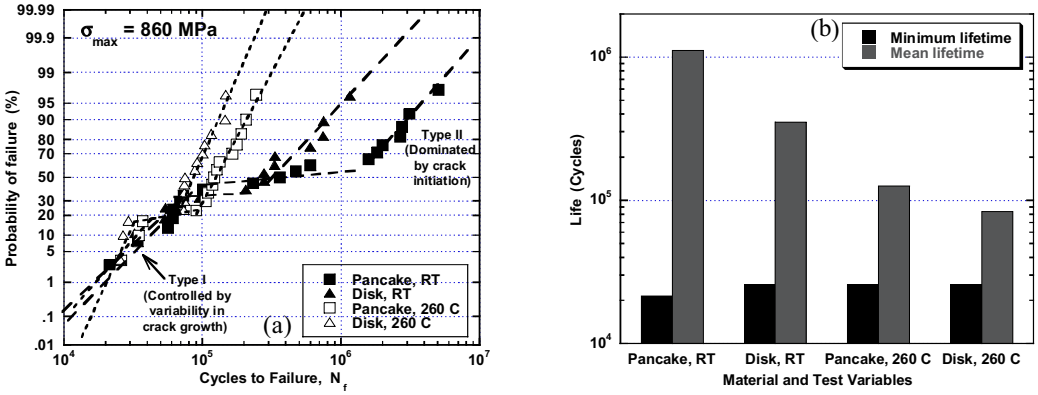

Figure 7: Effect of temperature on the fatigue variability behavior of Ti-6-2-4-6; (a) Illustrating the shift in the Type II failures, while there is almost no change in the Type I distribution with microstructure and temperature, and (b) The minimum vs. the mean behavior.

New Paradigm for Fatigue Variability Behavior

As discussed previously, the conventional understanding of the mean fatigue response to microstructure and loading variables may not be adequate to describe the fatigue variability behavior. This calls for an alternate framework to evaluate fatigue variability, especially from the perspective of design life prediction. Based on our analysis of the fatigue variability behavior of Ti-6-2-4-6 and other materials [10, 11], we hypothesize that the mean behavior is dominated by a different mechanism than the one controlling the lower-tail behavior. Therefore, given a theoretically sufficient number of trials, the fatigue variability behavior will be composed of a worst-case mechanism that is governed by purely the variability in small + long crack growth and a superimposing mechanism that follows the conventionally expected response to operating variables. Microstructure and loading variables will therefore have separate influences on the mean and the worst-case response. Clearly, the theoretical possibility of this effect may not be realized in practice in all cases, depending on the probabilities of occurrence of each mechanism. Nevertheless, this paradigm calls for a probabilistic assessment of the separation of lifetimes into mechanisms.

With respect to the Ti-6-2-4-6 pancake material, the increase in crack initiation lifetime with decreasing stress level, while at the same time a much lower sensitivity of the crack growth lifetime to stress level, will increase the separation between Type I and Type II mechanisms. causing an increase in total variability (Fig. 2(a)). Also, depending on the sensitivity of the crack initiation and the growth regimes to microstructure and temperature, the Type I and II mechanisms are affected differently, leading to shift in the mean and the total variability in fatigue lifetime. The behavior at 1040 MPa (Fig. 2(a) and 2(c)) can be viewed as a result of overlap between the two mechanisms, due to the crack initiation lifetime being reduced to zero. The amount of overlap between Type I and II mechanisms will also vary with material modifications that alter the deformation behavior, therefore affecting crack initiation and growth to different degrees.

Simulation of Variability in the Type I Mechanism

A Monte Carlo simulation of fatigue variability was conducted using the key controlling factors, i.e., the distribution in the crack initiation size and the variability in crack growth behavior. The distribution in the crack initiation size is shown in Fig. 8 (a). The data can be fit by the lognormal distribution function as shown in the figure. The small crack growth behavior was approximated by a relationship of the same form as the Paris-law equation:

$$\frac{da}{dN} = e^{c}\Delta K^{m} \tag{1}$$

where c and m are the small crack growth parameters. This relationship is often used to describe the average small-crack growth behavior, especially when the fluctuations in growth rates are small [33, 34]. The parameters c and m have been shown to be distributed normally, both in case of the long-crack [35] and the small-crack growth [34], and the same assumptions were employed here. The $\pm 3\sigma$ points of the distributions of m and c were taken to correspond to the small-crack growth limits shown in Fig. 5(a). The resulting distribution functions describing the variability in m and c are shown in Fig. 8(b). Since the parameters m and c are correlated [34, 35], these were sampled from their joint probability density using the algorithm given in [35]. The long-crack growth behavior was treated deterministically, since the variability in that regime was not significant. The cycles to failure, N_f, is given by:

$$N_f = \int_{a_i}^{a_0} \frac{da}{e^{c}\Delta K^{m}} + \int_{a_0}^{a_f} \frac{da}{e^{c_l}\Delta K^{m_l}} \tag{2}$$

The first and the second term in Eqn. (2) correspond to the small- and the long-crack regimes, respectively. The parameter, a_i is the starting crack size, which is derived from the crack initiation area; a_o is the crack length corresponding to the point of intersection of the small and the long crack growth curves and varies depending on the values of m and c; a_f is the final crack size measured from a fracture surface. The constants c_l, and m_l correspond to the long-crack growth equation.

The simulated lifetimes for the σ_{max} level of 860 MPa are compared to the experimental data in Fig. 9(a). As shown, the range in simulated lifetimes is similar to that of the Type I failures. The Type I failures, i.e., those belonging to the rising part of the step, are plotted as a separate distribution in Fig. 9(b). The intermediate points that form the horizontal part of the step, presumably due to some overlap between the mechanisms, have not been included. The figure illustrates that the variability in simulated lifetimes are in reasonable agreement with the variability in the Type I failures. Therefore, the uncertainty in the Type I mechanism can be determined by simulation of the lifetime related to variability in the relevant microstructure size scale and in the small-crack growth.

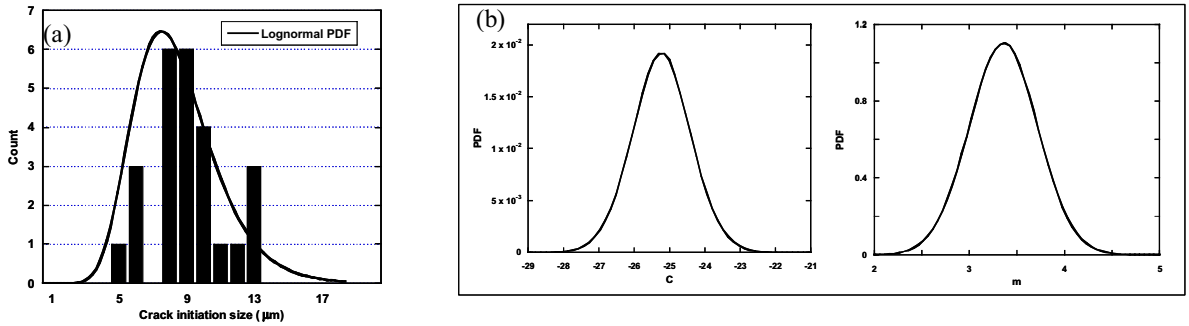

Figure 8: Inputs of the Monte Carlo simulation; (a) variability in the crack initiation size, and (b) variability in the small-crack growth behavior.

Implications for Design Life Prediction

With respect to life prediction, the new paradigm can significantly reduce the uncertainty in design life associated with the traditional approach. As shown in Fig. 9 (b), the total uncertainty breaks down into the variability in the Type I and the Type II mechanisms, with some degree of overlap between the two. Since failure can occur by either one of the mechanisms, life prediction can be based on the uncertainty in the worst-case failure (Type I), i.e., variability in small + long crack growth from the relevant size scale. This is illustrated in Fig. 9(b). A significant reduction in uncertainty and improvement in the utilization potential can be achieved, as indicated in the figure at the probability of failure of 0.1 (the 1 in 1000 criterion typically used for fracture critical components [2]). As we show in another paper in these proceedings [11], besides reducing the uncertainty, this methodology may enable more reliable design life. This is because; the approach based on an extrapolation of the variability about the overall mean behavior may inadvertently

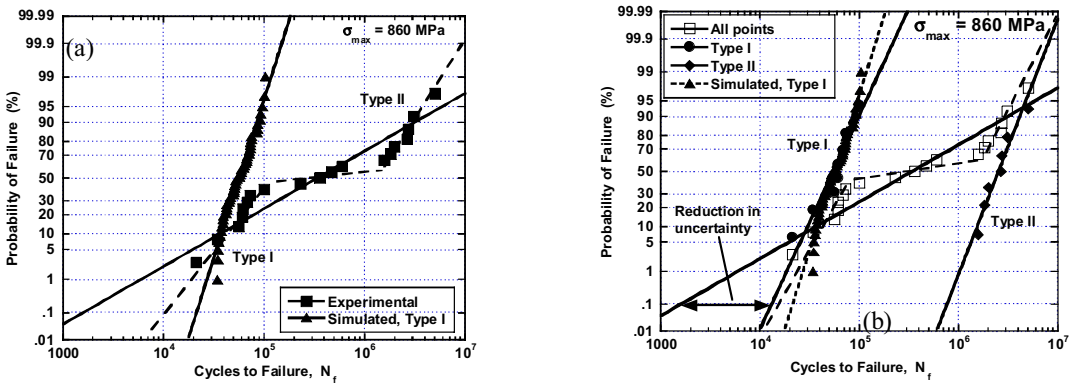

Figure 9: (a) Simulated lifetime compared to the experimental points, and (b) illustration of the life prediction methodology based on the new paradigm of fatigue variability behavior.

cause the worst-case behavior to be overlooked if the mean has an extreme bias towards longer lifetimes [11]. The predicted design life, in that case, may be non-conservative with respect to the minimum observed lifetime [11]. Since the new approach is based on the variability in the mechanism controlling the lower tail behavior, it effectively accounts for this possibility.

CONCLUSIONS

The study of the fatigue variability behavior of the Ti-6-2-4-6 alloy with respect to microstructure and temperature revealed, perhaps, some fundamental aspects of fatigue variability that cannot be described by the conventional understanding. We proposed a new paradigm for the fatigue variability behavior in which the mean fatigue-lifetime behavior is thought to be dominated by a different mechanism than the one controlling the worst-case behavior. This causes the worst-case and the mean behavior to respond differently to changes in microstructure, stress level, and other loading variables. Further, we find that the worst-case behavior is controlled by the variability in the small + long crack growth, starting from the relevant size scale.

With respect to the present Ti-6-2-4-6 material, most of the contribution to fatigue variability was realized in crack initiation and small-crack growth occurring on the order of the primary α_p size. The mean lifetime behavior was increasingly dominated by crack initiation with decreasing stress level, which caused increased separation between the mean and the worst-case behavior, since the latter was controlled by crack growth.

The change in microstructure from pancake to disk shifted the crack initiation controlled mechanism, while the worst-case failure distribution remained almost unaffected. This led to a decrease in the mean lifetime as well as the total variability, but there was no statistically identifiable effect of the microstructural differences on the minimum (worst-case) fatigue lifetimes of these two heats of material. This was attributed to the strong sensitivity of the crack initiation regime to the change in texture, while there appeared to be an almost insignificant effect of the on the crack growth behavior.

The increase in temperature to 260ºC caused a further shift to lower lifetimes in the crack initiation controlled mechanism for both microstructures. At the same time, the worst-case distribution did not vary in any statistically significant way. This again produced a decrease in the overall mean lifetime and also in the total variability in lifetime. This was related to the different degrees of influence of temperature on the crack initiation and the growth regimes.

The proposed paradigm was implemented in a life prediction methodology and shown to significantly decrease the uncertainty in the predicted life associated with the traditional approach. The methodology precludes the inaccurate assumption that the fatigue variability behavior can be described by the variability about the overall mean behavior, but rather evaluates life based on the variability in the worst-case behavior. As a result, this methodology may also improve the reliability of design life, since the cases where the mean has an extreme bias towards the long-life mechanism (therefore producing overly conservative predictions with respect to the worst-case behavior) are treated effectively.

REFERENCES

1. Suresh, S. *Fatigue of Materials*, Cambridge University Press, 1991.
2. Christodoulou, L., and Larsen, J. M. (2004) *JOM* March, 15.
3. DeBartolo, E. A., and Hillberry, B. M. (2001) Int. J. Fatigue 23, S79.
4. Tryon, R., and Dey, A. (2001) *J. Aerospace Engng.* Oct, 120.
5. de Bussac, A. and Lautridou, J. C. (1993) *Fatigue Fract. Engng. Mater. Struct*. 16, 861.
6. Goto, M. (1994) *Fatigue Fract. Engng. Mater. Struct*. 17, 635.
7. Jha, S. K., Larsen, J. M., Rosenberger, A. H., and Hartman, G. A. (2003) *Scripta Materialia* 48, 1637.
8. Jha, S. K., Larsen, J. M., and Rosenberger, A. H. (2005) *Acta Materialia* 53, 1293.
9. Jha, S. K., Larsen, J. M., and Rosenberger, A. H. (2005) *JOM* Sep, 50.
10. Caton, M. J., Jha, S. K., Larsen, J. M., and Rosenberger, A. H. In: Superalloys 2004.
11. Jha, S. K., Caton, M. J., Porter, W. J., Li, K., Larsen, J. M., and Rosenberger, A. H. In: Fatigue 2006.
12. Boyer, R. R. (1996) *Mater. Sci. Engng.* A213, 103.
13. Honnorat, Y. (1996) *Mater. Sci. Engng.* A213, 115.
14. Cowles, B. A. (1988) *Mater. Sci. Engng.* A103, 63.
15. Neal, D. F., and Blenkinsop, P. A. (1976) *Acta Metall*., 24, 59.

16. Hall, J. A. (1997) *Int J. Fatigue*, 19, S23.
17. Lutjering, G. (1999) *Mater. Sci. Engng.*, A263, 117.
18. Mahajan, Y., and Margolin, H. (1982) *Metall. Trans.*, 13A, 257.
19. Kruzic, J. J., Campbell, J. P., and Ritchie, R. O. (1999) *Acta Materialia*, 47, 801.
20. Rosenberger, A. H., Worth, B. D., and Larsen, J. M. (1997) In: *Structural Intermetallics*, TMS Publications, 555.
21. Shyam, A., Torbet, C, J., Jha, S. K., Larsen, J. M., Caton, M. J., Szczepanski, C. J., Pollock, T. M., and Jones, J. W. (2004) In: Superalloys 2004.
22. Ruppen, J., Eylon, D., and McEvily, A. J. (1980) *Metall. Trans.* 11A, 1072.
23. Chait, R. and DeSisto, T. S. (1977) *Metall. Trans.* 8A, 1017.
24. Atrens, A. Hoffelner, W., Duerig, T. W., and Allison, J. E. (1983) *Scripta Metallurgica* 17, 601.
25. Yi, J. Z., Gao, Y. X., Lee, P. D., Flower, H. M., and Lindley, T. C. (2003) *Metall. Mater. Trans*. 34 A, 1879.
26. Jha, S. K., Larsen, J. M., and Rosenberger, A. H., to be published.
27. Kendall, D. P. (1986) *Trans. ASME* 108, 490.
28. Skallerud, B., Iveland, T., and Harkegard, G. (1993) *Engng. Fract. Mechanics* 44, 857.
29. Foreman and Shivakumar, ASTM STP
30. Jha, S. K., Larsen, J. M., and Rosenberger, A. H., Materials Damage Prognosis, 2004.
31. Szczepanski, C. J., Jha, S. K., Larsen, J. M., and Jones, J. W., Fatigue 2006.
32. Jha, S. K., Larsen, J. M., and Rosenberger, A. H., to be published.
33. Bruckner-Foit, A.,Jackels, H., and Quadfasel, U. (1993) *Fatigue Fract. Engng. Mater. Struct.* 16, 891.
34. Luo, J. and Bowen, P. (2003) *Acta Materialia* 51, 3521.
35. Annis, C. J., Probabilistic aspects of life prediction, ASTM STP 1450, 2004.